International Conference on Applied Energy 2019
Aug 12-15, 2019, Västerås, Sweden
Paper ID: 329

NUMERICAL INVESTIGATION ON THE EROSION PROCESS OF HYDRATE MATERIALS USING WATER JET

Yiqun Zhang*, Kexian Zhao, Gensheng Li, Xiaodong Hu, Xiaoya Wu

China University of Petroleum (Beijing)

ABSTRACT

Natural gas hydrate (NGH) is a potential fuel resource. Radial Jet Drilling (RJD), turning sharply in the casing and drilling laterals by using water jet, is a valid approach to solve problems of high cost, low efficiency and formation collapse during the exploitation of NGH resources in permafrost and continental margins. Traditional finite element methods, which tend to produce mesh distortion, cannot accurately depict the water jet drilling efficiency. This paper presents a numerical investigation of Arbitrary Lagrangian Eulerian (ALE) method for analyzing both NGH and Hydrate-bearing Sediments (HBS) erosion process using water jet. Firstly, a coupled nozzle-target model is solved by ALE method. The material constitutive models are established based on the characteristics of water, NGH and HBS. After that, several case studies are conducted in air, submerged water and confining pressure environments (different working conditions). Not only the flow field, but also the deformation and erosion of the materials induced by water jet are estimated. Finally, the simulation results, such as damage field, variation of internal material stress and erosion pit characteristic, are compared with each other. The relation curves between erosion depth and hydraulic parameters are consistent with the experimental results. The results show that the ALE method can better simulate the water jet flow field, by which the water jet rock breaking simulation is more in line with the reality and accurately predict the fracture result. Additionally, water jet has obvious destructive/damage effect on NGH and HBS, the presence of confining pressure will inhibit the breaking of materials.

Keywords: Natural gas hydrate, Water jet, Erosion, Numerical simulation, Arbitrary Lagrangian Eulerian method

1. INTRODUCTION

NGH is composed mainly of a white crystalline solid substance, which is formed by the interaction of water and methane with a high pressure and low temperature environment[1]. At present, common methods of NGH production include depressurization, thermal stimulation, inhibitor injection and CO2 replacement[2]. No matter which production method we select, the first step of utilizing NGH is to quickly drill into reservoirs and establish stable wellbores. Moreover, the solid fluidization exploitation method aims to break NGH ore body into small particles and transport the particles through a riser. Water jet is an efficient method of rock breaking, especially for soft sediments erosion[3]. Therefore, the authors believe that RJD technology[4],[5] of jet side tracking with coiled tubing has great potential. Fig 1 illustrates the application of multi-lateral wells in marine gas hydrate production, where multi-laterals in different depth are drilled by water jet to form the "highway network" of hydrocarbon migration. The contact area can be extremely increased.

The previous simulation and experiment studies have made significant contributions to analyze the water jet erosion process on different materials. Zhao[6] and Mabrouki[7] used different methods to simulate the process of water jet breaking rock. Pernas-Sánchez[8] and Combescure[9] respectively carried out numerical simulation and experiment on the process of high-speed impact ice. Xue[10] simulated water jet erosion coal under confining environments. However, almost all simulations cannot reflect the actual operation condition. Without taking into account the presence of the flow field, water jet is usually simplified into a water column of constant velocity, which neglects the action of the nozzle. Based on the in-situ acoustic logging data of Clyato[11] and Luo[12], Ning[13] studied the mechanical properties of HBS in the South China Sea. Numerical

Selection and peer-review under responsibility of the scientific committee of the 11th Int. Conf. on Applied Energy (ICAE2019).

simulation of water jet erosion HBS, which analyzed the influence of nozzle (water column) diameter and jet velocity on the depth and diameter of the erosion pit, was carried out by Chen[14].

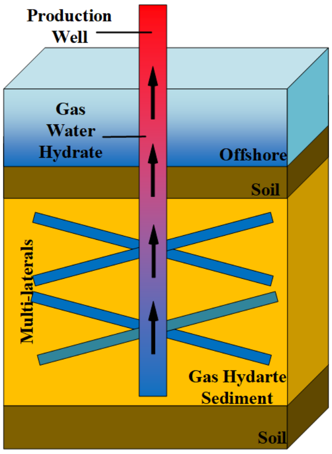

Fig 1 Schematic diagram of natural gas hydrate production by multi-lateral wells

2. MATERIAL OF WATER JET EROSION

2.1 Water material model

A rich library of materials is built into Ls-Dyna to meet the needs of most numerical simulations. MAT_NULL and EOS_GRUNEISEN are used together to describe the motion process of water in this study. Water is considered as a completely plastic material, and the Mie-Grueisen equation[15] of state is used.

2.2 NGH material model

Cox[16] and Dvorkin[17] compared the physical properties of hydrate and ice. Yu[18] reviewed previous study and concluded that the mechanical properties of ice and NGH are similar. Therefore, the constitutive equation of NGH can be replaced by the constitutive equation of ice to simplify the model.

MAT_ISOTROPIC_ELASTIC_FAILURE is a constitutive model commonly used to describe ice. It belongs to the model of isotropic plastic damage. This model is suitable for high strain conditions under water jet impact. The specific parameters are listed in Table 1.

Table 1 Material parameters of NGH

Density	Shear modulus	Yield stress	Plastic modulus
910 kg/m3	2.20 GPa	2.12 MPa	4.26 GPa
Bulk modulus	Plastic failure strain	Failure pressure	
5.26 GPa	0.35	-4 MPa	

2.3 HBS material model

MAT_FHWA_SOIL is a constitutive model commonly used to describe soil. It belongs to the nonlinear elastoplastic isotropic damage material model[19] and follows an improved Mohr-Coulomb rule. The specific parameters are listed in Table 2.

Table 2 Material parameters of HBS

Density	Specific gravity	Bulk modulus	Shear modulus
2000Kg/m3	2.7	9.2GPa	4.5GPa
Cohesion	Moisture content	Friction angle	
0.6MPa	0.5	0.218rad	

3. MODEL DESCRIPTION

The ALE description combines the advantages of both the pure Lagrangian description and the pure Eulerian description[20]. In the ALE description, the grid points are neither constrained to remain fixed in space nor to move with material. In fact, the grid points can be moved arbitrarily independent of the underlying material and have their own motion governing equations. ALE is a great method to solve the fluid-solid coupling problems like water jet breaking NGH or HBS. As illustrated in Fig 2, part 1 and 3 are set to ALE mesh, while part 2 and 4 are set to Lagrangian mesh.

3.1 Calculation model establishment

Assuming that the water jet erosion process only exists mechanical actions, the hydrates do not decompose and phase transitions do not occur. The simplified physical model is shown in Fig 2.

A 1/4 3D model is established for simplified calculation and direct observation. The geometric dimensions of the model are as follows, air size is 42×42×71mm, water column size in the tube is 10mm×10 mm, natural gas hydrate/hydrate sediment geometry model size is 40×40×50 mm, the nozzle outlet diameter is 2mm, the nozzle wall thickness is 1mm, the standoff distance is 20mm, and the nozzle has a contraction length of 8mm.

In order to improve the calculation accuracy, the partial meshes shown in Fig 2 are optimized (smoothly mapped from a cylinder to a cube). The ALE mesh and Lagrangian mesh are coincident to reduce the possibility of excessive iterations.

3.2 Constraints and boundary conditions

Constraining the degree of freedom of the nozzle and the bottom of NGH/HBS, giving the water in pipeline a downward initial velocity and setting the hydrates. Air and NGH/HBS boundaries are set to a non-reflective condition[21].

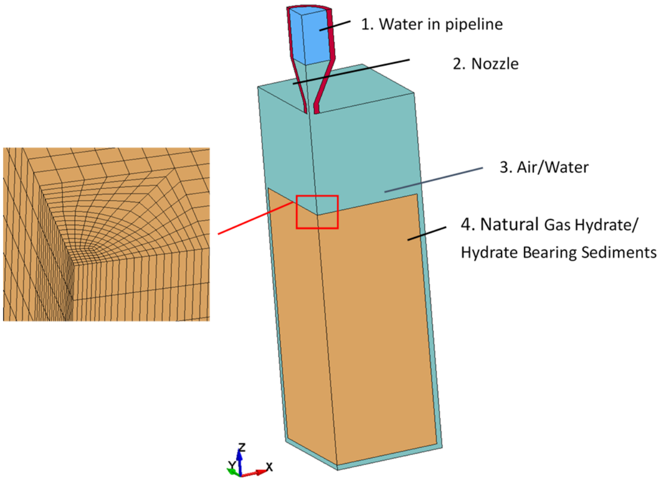

Fig 2 Model of all parts

4. RESULTS AND DISCUSSION

4.1 Flow field

The initial velocity is 6m/s, the diameter of the column is 10mm, the nozzle diameter is 2mm, and the nozzle outlet speed should be 150m/s. The velocity in Fig 3 is basically in line with the calculation, and the flow field can be observed.

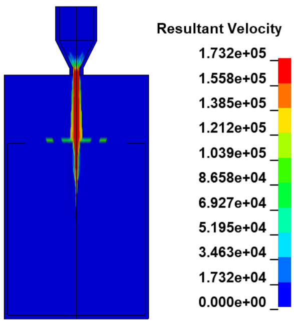

Fig 3. Speed distributions during NGH erosion process at 12×10^{-5}s (speed unit: mm/s)

4.2 Water jet erosion of NGH

Fig 4 shows the process of NGH erosion with cracks generated, and the size of the erosion pit and the crack gradually increases. Radius, depth of pit and crack width data are marked, and the crack width is 14.45mm at 60×10^{-5}s. The direction of the crack is about 37° with the positive direction of the Y-axis. (To ensure the consistency of the coordinate axes, the start time is set to the moment when the NGH begins to be broken, the same below) The large NGH ore body could be broken into small particles by water jet, which in turn prove the feasible of the solid fluidization exploitation method.

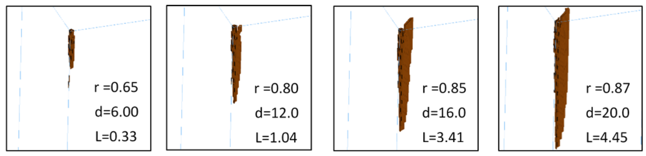

(a)$t=6\times10^{-5}$s (b) $t=9\times10^{-5}$s (c) $t=12\times10^{-5}$s (d) $t=15\times10^{-5}$s

Fig4. Eroded part of NGH by water jet (pit radius, r; pit depth, d; crack width, L; unit, mm)

To investigate the effects of standoff distance (only the control group has a standoff distance of 1cm and the other is 2cm, the same below), submergence conditions, and submerged confining conditions on the results, multiple models are set to contrast.

As shown in Fig 5, the model with a short standoff distance has a strong damaging effect on the hydrate, and erosion volume increase rate of the erosion pit is faster; in the later stage, the other one with larger standoff distance generates a bigger pit and crack, leading to the larger erosion volume.

In submerged environment, due to the existence of the nozzle structure, a gradually accelerating water jet is generated in the initial stage, which causes the NGH to be destroyed first to form an erosion pit without cracks before 21×10^{-5}s; after that the water reached the highest speed contacts the NGH, then the crack begins to generate and expand, resulting in a rapid increase in erosion volume.

Compared with the air environment, the actual erosion time in submerged condition is much longer, resulting in an approximate erosion volume (black and blue curves in Fig 5). And the crack generated in the submerged condition extending along the x,y axis, which is different from the Fig 4. It may be related to the characteristics of submerged jet turbulent flow field.

In order to investigate the influence of confining pressure on hydrate rocks breaking, the pressure of 5 MPa is applied to the surrounding surface of the NGH (target model) under submerged conditions. Because the erosion pits with cracks are generated in both submerged condition and submerged confining condition, the green and blue curves (erosion volume versus time) look almost coincide as illustrated in Fig 5. It indicates the existence of confining pressure could hardly limit the generation of cracks.

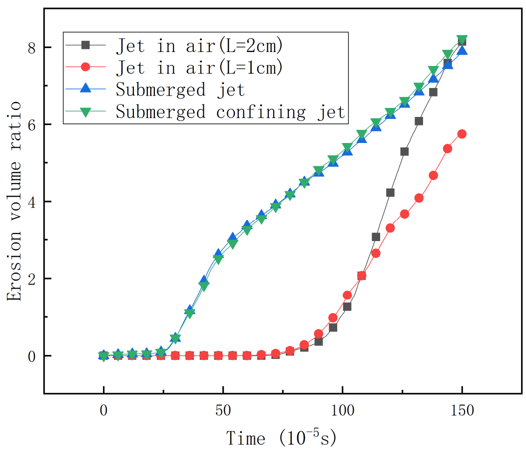

Fig 5 Erosion volume ratio of NGH versus time under different working conditions

The influence of the jet velocity on NGH erosion efficiency under submerged confining condition is investigated as shown in Fig 6. The nozzle outlet speed within potential core region ranges from 50.0m/s to 150.0m/s. It is found that the NGH erosion efficiency increases with the increase of jet velocity and there are two types of growth rates of erosion volume -- high speed jet with cracks generated and low speed jet erosion. Especially, the erosion volume of 50.0m/s jet velocity change slowly within 1ms (early stage) and then increase gradually, which indicates the erosion pit without cracks is generated.

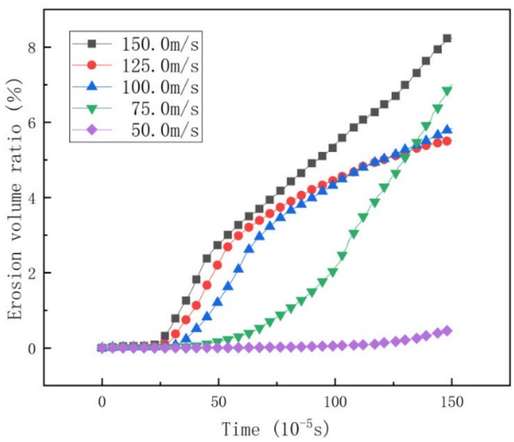

Fig 6 Erosion volume ratio of NGH versus time under different jet velocity

4.3 *Water jet erosion of HBS*

The jet velocity within potential core region is set to 100m/s for the soil model of HBS. Fig 7 shows the HBS damage field and stress cloud map distribution at different times. No cracks are generated with gradual increase of the depth (8.7 to 38.2mm) and radius (1.1 to 2.4mm) of the erosion pit. Since the standoff distance is not small enough, the jet does not cause erosion damage inside the erosion pit, and no large cavity is formed[22].

The stress distribution in Fig 7 is mainly concentrated on the cone-shaped area at the bottom of the erosion pit, making the erosion pit continue to stretch. As the bottom of the pit is in a critical state of failure, the stress distribution cannot be reflected in the graph.

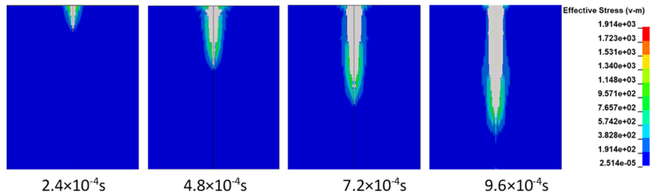

Fig 7 Damage field and effective stress field distribution of HBS (unit of color bar: MPa)

The depth of the erosion pit produced by water jet with a short standoff distance is consistently greater than the other as shown in Fig 8(a). However, the final erosion volume showing in Fig 8(b) with a short standoff distance is smaller than the other since it generates a slender erosion pit, and due to the existence of the flow field at the nozzle outlet, the erosion pit with larger standoff distance has larger radius and volume finally.

Similar to 4.2, 20MPa of confining pressure are applied to contrast the influence of it. As shown in Fig 8(b), both of submergence and confining conditions can hinder the erosion efficiency of water jets. In submerged environment, the higher the confining pressure, the more difficult it is to damage HBS, as shown in Fig 8(c).

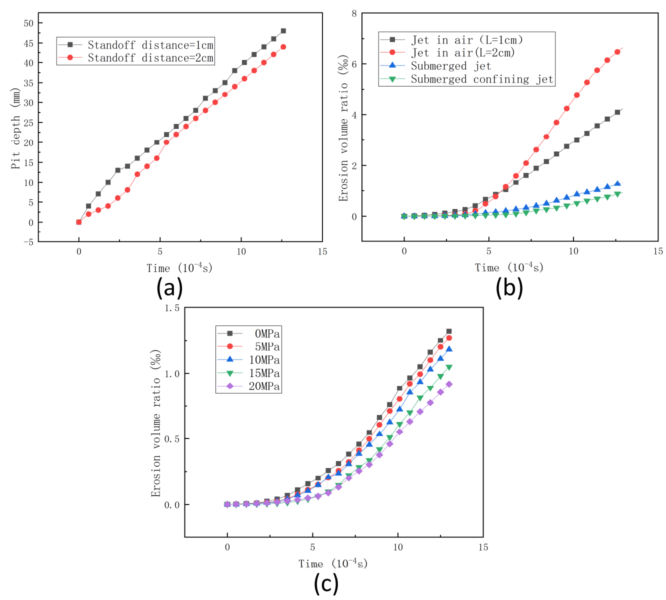

Fig 8 (a) Erosion depth with different standoff distance
(b) Erosion volume of HBS under different working conditions
(c) Erosion volume of HBS under different confining pressure

The influence of the jet velocity on HBS erosion efficiency is also investigated as shown in Fig 9. The pressure of 5 MPa is applied to the surrounding surface of the HBS under submerged conditions. The nozzle outlet speed within potential core region is set as 50.0m/s, 62.5m/s, 75.0m/s, 87.5m/s and 100.0m/s respectively. It is found that the HBS erosion efficiency increases with the increase of jet velocity. Particularly, the purple curve represents that the erosion volume ratio is slightly above 0‰ within 1.5ms. Therefore, we regard the threshold velocity, which is the minimum jet velocity to break the HBS, as 50.0m/s in this situation.

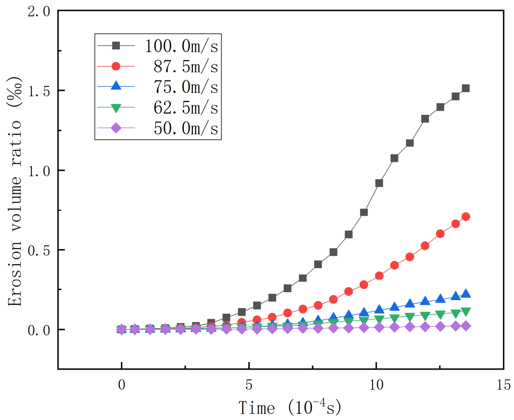

Fig 9 Erosion volume ratio of HBS versus time under different jet velocity

5. CONCLUSIONS

(1) The ALE method can well simulate the water jet flow field, by which the water jet rock breaking simulation is more in line with the reality and accurately predict the erosion result.

(2) The water jet has noticeable damage effect on NGH, and there is obvious crack growth. The presence of confining pressure could hardly limit the generation of cracks, but the decrease of jet velocity will inhibit growth of cracks.

(3) The water jet also has obvious damage effect on HBS under submerged confining conditions. The larger the confining pressure, the weaker the erosion effect. Additionally, the existence of the threshold velocity for HBS erosion is proved.

ACKNOWLEDGEMENT

The study was supported by the National Natural Science Foundation of China (51804320).

REFERENCE

[1] Y. F. Makogon, S. A. Holditch, and T. Y. Makogon, “Natural gas-hydrates - A potential energy source for the 21st Century,” J. Pet. Sci. Eng., vol. 56, no. 1–3, pp. 14–31, 2007.

[2] Y. Konno et al., “Key Findings of the World’s First Offshore Methane Hydrate Production Test off the Coast of Japan: Toward Future Commercial Production,” Energy and Fuels, vol. 31, no. 3, pp. 2607–2616, 2017.

[3] H. Z. Kuyumcu and L. Rolf, “Application of high-pressure waterjets for comminution,” Int. J. Miner. Process., vol. 74, no. SUPPL., pp. 191–198, 2004.

[4] J. Ren et al., “Multi-branched horizontal wells for coalbed methane production: Field performance and well structure analysis,” Int. J. Coal Geol., vol. 131, pp. 52–64, 2014.

[5] S. Tian, Z. Huang, G. Li, P. Lu, H. Zhang, and T. Wang, “Laboratory experiments on blockage removing and stimulation of CBM reservoirs by composite pulsating hydraulic fracturing of radial horizontal wells,” Nat. Gas Ind. B, vol. 6, no. 2, pp. 151–158, 2019.

[6] J. Zhao, “Mechanism and effect of jet parameters on particle waterjet rock breaking,” Powder Technology, vol. 313. pp. 231–244, 2017.

[7] T. Mabrouki, K. Raissi, and A. Cornier, “Numerical simulation and experimental study of the interaction between a pure high-velocity waterjet and targets: Contribution to investigate the decoating process,” Wear, vol. 239, no. 2, pp. 260–273, 2000.

[8] J. Pernas-Sánchez, D. A. Pedroche, D. Varas, J. López-Puente, and R. Zaera, “Numerical modeling of ice behavior under high velocity impacts,” Int. J. Solids Struct., vol. 49, no. 14, pp. 1919–1927, 2012.

[9] A. Combescure, Y. Chuzel-Marmot, and J. Fabis, “Experimental study of high-velocity impact and fracture of ice,” Int. J. Solids Struct., vol. 48, no. 20, pp. 2779–2790, 2011.

[10] Y. Xue, H. Si, Z. Yang, and D. Xu, “Microscopic damage field in coal induced by water jets,” J. Loss Prev. Process Ind., vol. 56, no. November 2017, pp. 300–315, 2018.

[11] C. R. I. Clayton, J. A. Priest, and A. I. Best, “The effects of disseminated methane hydrate on the dynamic stiffness and damping of a sand,” Géotechnique, vol. 55, no. 6, pp. 423–434, 2005.

[12] T. Luo et al., “Triaxial experiments on the mechanical properties of hydrate-bearing marine sediments of South China Sea,” Mar. Pet. Geol., vol. 77, pp. 507–514, 2016.

[13] F. NING et al., “Estimation of in-situ mechanical properties of gas hydrate-bearing sediments from well logging,” Pet. Explor. Dev., vol. 40, no. 4, pp. 542–547, 2013.

[14] C. Chen et al., “Investigation into the Water Jet Erosion Efficiency of Hydrate-Bearing Sediments Based on the Arbitrary Lagrangian-Eulerian Method,” Appl. Sci., vol. 9, no. 1, p. 182, 2019.
[15] F. Wang, R. Wang, W. Zhou, and G. Chen, “Numerical simulation and experimental verification of the rock damage field under particle water jet impacting,” International Journal of Impact Engineering, vol. 102. pp. 169–179, 2017.
[16] John L Cox, “Natural gas hydrates: properties, occurrence and recovery,” Boston:Butterworth, 1983.
[17] J. Dvorkin, M. B. Helgerud, W. F. Waite, S. H. Kirby, A. Nur, “Introduction to Physical Properties and Elasticity Models. In: Max M.D. (eds) Natural Gas Hydrate. Coastal Systems and Continental Margins,” vol 5. Springer, Dordrecht, 2000.
[18] Yibing Yu, Fulong Ning, Guosheng Jiang, Ling Zhang, “Mechanical behavior of pure hydrates,” Advances in Mechanics, vol. 42. pp. 347-358, 2012.
[19] J. D. Reid, B. A. Coon, B. A. Lewis, S. H. Sutherland, and Y. D. Murray, “Evaluation of LS-DYNA Soil Material Model 147,” Report, no. November, p. 85, 2004.
[20] L. B. Zhang, and Z. X. Cai, “A novel approach for simulation of soil-tool interaction based on an arbitrary Lagrangian–Eulerian description,” Soil Tillage Res., vol. 178, no. July 2017, pp. 41–49, 2018.
[21] X. Liu, S. Liu, and H. Ji, “Numerical research on rock breaking performance of water jet based on SPH,” Powder Technology, vol. 286. pp. 181–192, 2015.
[22] Yang Lin, “Study on the breaking process of marine hydrate reservoirs subjected to high pressure water jet and the production increase of marine hydrate reservoirs reconstruction,” PhD Diss., Jilin University, 2018.